The bridged crack model for reinforced concrete elements with a nonlinear matrix

Alberto Carpinteri, Giuseppe Ferro & Giulio Ventura
Politecnico di Torino, Torino, Italy

ABSTRACT: A Fracture Mechanics method for reproducing the constitutive flexural response of a reinforced concrete element with a nonlinear matrix is proposed. The nonlinearity of the matrix is modelled by considering a distribution of closing forces onto the crack faces which increases the fracture toughness of the cross-section with a shielding action. In order to take into account these closing forces, a dimensionless formulation of the bridged crack model is proposed, as well as its cohesive version. The constitutive flexural response depends on three dimensionless parameters: $\tilde{w}_c{}^E$, which controls the extension of the process zone, $N_P{}^{(1)}$ and $N_P{}^{(2)}$, called *brittleness numbers*, which are related to the reinforcement phases. The role of the specimen size scale is fundamental for the global structural behaviour, which can range from ductile to brittle simply with the variation of the two brittleness numbers. The numerical curves for such a case are presented, with all the mechanical parameters fixed and varying only the specimen size.

1 INTRODUCTION

In the last few years, growing attention for cementitious-matrix composite materials has been evidenced, in relation to the use of high-strength concretes. A primarily incentive in using fibers is to cut production costs by reducing, where possible, the cross-section of the element or eliminating some forms of conventional reinforcement. Recent research has confirmed the possibility to replace stirrups with fibers in high-strength concrete beams. On the other hand, what discourages the use of fibers in concrete is a lack of guidelines for design of structural elements made of fibrous concrete. In order to obtain a desired structural effect, an optimal combination of fibers, bars and concrete must be chosen. Moreover, the high strength of concrete and the high percentage of primary reinforcement normally adopted in the element make the experimental tests impossible at full scale with the standard jacks available in the laboratory. The tests are normally realized on specimens reduced in size. This aspect appears strategical, strongly size-scale effects being present. How to approach this problem is one of the main goals of the present paper.

The proposed theoretical model determines the problem unknowns by considering a cracked cross section in bending and by using the local compliance and the stress-intensity factor concepts for reinforced concretes with a nonlinear matrix. It represents an extension of the model proposed by Carpinteri (1984) and by Bosco and Carpinteri (1995) for a discontinuous fiber distribution and by Carpinteri and Massabò (1997a) for a continuous one. The longitudinal reinforcements are simulated by the actions of *m* concentrated forces directly applied onto the crack faces. The nonlinearities of the matrix are modelled by the action of a continuous closing traction distribution onto the crack zone whose opening displacements result less than the critical value, w_c.

From Dimensional Analysis, the structural response, expressed by the functional relationship of moment versus local rotation, i.e. M vs ϕ, comes out to depend on three dimensionless parameters. The first parameter, $\tilde{w}_c{}^E$, is the product of the dimensionless Young's modulus by the normalized critical crack opening displacement. The other two parameters, $N_P{}^{(1)}$ and $N_P{}^{(2)}$, called *brittleness numbers*, are related to the geometry and to the mechanical characteristics of reinforcements and matrix. The structural response depends, once all the other mechanical parameters have been set, on the structural element dimension.

Theoretical results confirm a transition from brittle to ductile collapse by varying the brittleness numbers N_P. It is to be observed that the dependence of the brittleness numbers on the structural dimension is represented by a power law with an exponent equal to 0.5, typical for the LEFM stress singularity.

2 THEORETICAL MODELS

The theoretical model explains and reproduces the constitutive flexural response of a fiber-reinforced concrete element with longitudinal steel bars. Two different options for the model can be used, the *bridging* and the *cohesive*. The scheme of a cracked element is shown in fig.1, where h and b are the height and the thickness of the cross-section. The normalized crack depth $\xi=a/h$ and the normalized coordinate $\zeta=x/h$ are defined, x being the coordinate related to the bottom of the cross-section. In the *bridging option*, the distribution of the discrete actions P_i and of the continuous closing tractions $\sigma(w)$, directly applied onto the crack faces, represent the physical bridging mechanisms respectively of the longitudinal bars (primary reinforcement) and of the fibers (secondary reinforcement), acting at two different scales. Let c_i be the coordinate of the ith reinforcement from the bottom of the beam, and $\zeta_i=c_i/h$ its normalized value. Function $\sigma(w)$ is a constitutive law and defines the relation between the bridging tractions, representative of the action exerted by the fibers onto the crack, and $w(x)$, the crack opening displacement at the generic coordinate x. In the simulation presented herein a perfectly-plastic law with vertical drop has been used for the fibers, fig. 3.b, even if more general laws could also be considered and have been implemented in the numerical code (fig. 3.c,d). The bridging forces of the secondary reinforcement act on the portion of the crack where the opening displacement is less than its critical value w_c, beyond which the closing tractions vanish (fig. 2). In the *cohesive option*, instead, the
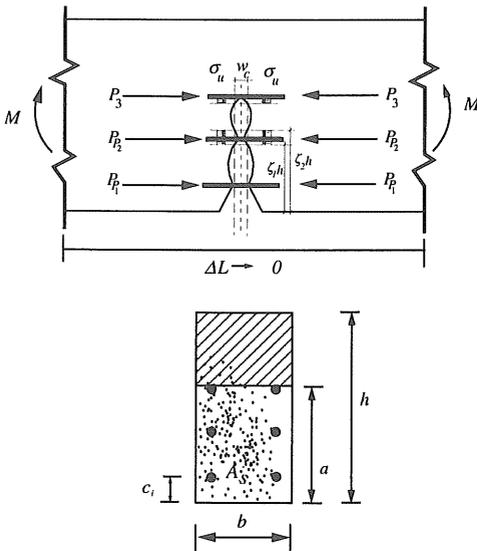
brittle matrix and the fibers are represented as a single-phase material with homogenized properties. In this case, the closing tractions $\sigma(w)$ describe the combined restraining action of matrix and fibers on the crack opening and are given by the cohesive law of the composite material.

The assumed rigid-plastic bridging relation for the crack opening displacement w_i at the level of the ith reinforcement is suitable to describe the yielding mechanism for the reinforcement as well as the bar-matrix relative slippage (fig. 3.a). The maximum bridging traction is defined for the primary reinforcements by the ultimate force $P_{Pi}=A_i\sigma_y$ and for the fibers by the ultimate stress $\sigma_0=\gamma\sigma_u$, A_i being the single reinforcement cross-section area, γ the fiber volume ratio, σ_y or σ_u the minimum between the reinforcement yield strength and the sliding limit for the two reinforcement phases. The stress-intensity factors K_{IM} due to the bending moment M, $K_{I\sigma}$ due to the fibers and K_{Ii} due to the ith-longitudinal reinforcement, can be expressed in accordance with the two-dimensional single-edge notched-strip solution:

$$K_{IM} = \frac{M}{bh^{1.5}}Y_M(\xi), \qquad (1)$$

where $Y_M(\xi)$ is a function of the relative crack depth ξ (Okamura et al., 1975; Tada et al., 1963). The factor $K_{I\sigma}$ is obtained by integrating, along the bridged crack zone, the product of the stress-intensity factor due to two opposite opening forces $P_j=1$, applied at the generic coordinate ζ_j, times the bridging actions $\sigma(w)$:

$$K_{I\sigma}=\int_0^\xi \frac{K_{Ij}}{P_j}\sigma(w(\zeta_j))bhd\zeta_j=\frac{1}{h^{0.5}}\int_0^\xi \sigma(w(\zeta_j))Y_P(\xi,\zeta)bhd\zeta_j \qquad (2)$$

where the integration is extended to the whole crack, while function $\sigma(w)$ assumes values different from zero only where $w<w_c$.
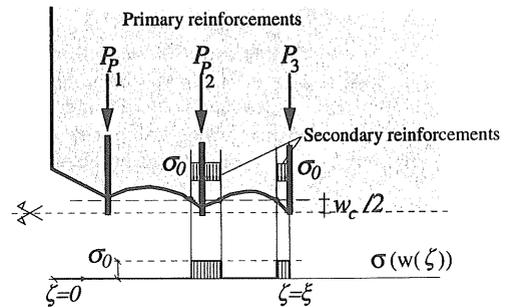

Figure 1. Scheme of a cracked reinforced concrete element containing fibers.

Figure 2. Bridging actions of primary and secondary reinforcements onto the crack faces and crack opening displacements.

For the ith longitudinal reinforcement we have:

$$K_{Ij} = \frac{P_i}{bh^{0.5}} Y_P(\xi, \zeta_i) \qquad i=1, 2,...., m \ , \tag{3}$$

where $Y_P(\xi, \zeta_i)$ is also function of the relative crack depth ξ. The crack propagates when K_I is equal to the matrix fracture toughness, K_{IC}, for the *bridging* option and when K_I vanishes for the *cohesive* one:

$$K_I = K_{IM} - \sum_{j=1}^{m} K_{Ij} - K_{I\sigma} = \begin{cases} K_{IC} & \text{bridging option} \\ 0 & \text{cohesive option} \end{cases} \tag{4}$$

The dimensionless crack propagation moment can be obtained from eqs (1-3):

$$\frac{M_F}{K_{IC}bh^{0.5}} = \frac{1}{Y_M(\xi)} \left\{ \frac{N_P^{(1)}}{\rho} \sum_{i=1}^{m} \rho \frac{P_i}{P_{P_i}} Y(\xi, \zeta) + \right. \tag{5}$$

$$\left. + N_P^{(2)} \int_0^\xi \frac{\sigma(w(\zeta))}{\gamma\sigma_u} Y_P(\xi, \zeta)bhd\zeta + K \right\}$$

with:

$$N_P^{(2)} = \frac{\gamma\sigma_u h^{0.5}}{K_{IC}} \quad \text{for K=1 (bridging option)} \tag{6}$$

$$N_P^{(2)} = \frac{1}{s} = \frac{\sigma_u h^{0.5}}{K_{IC}} \quad \text{for K=0 (cohesive option)}$$

where s is the brittleness number originally defined by Carpinteri (1981), and:

$$N_P^{(1)} = \frac{\rho\sigma_y h^{0.5}}{K_{IC}} \tag{7}$$

The parameters in the two cases assume different physical meaning. In the bridging option, K_{IC} represents the matrix fracture toughness while in the cohesive it represents the homogenized toughness of the composite; σ_u represents the ultimate strength of the secondary reinforcement in the former case or the homogenized ultimate strength in the latter. The localized rotation ϕ of the cracked cross-section can be evaluated by using Castigliano's Theorem:

$$\phi = \frac{\partial U_F}{\partial M} \ , \tag{8}$$

where U_F is the strain energy of the body due to the introduction of the crack. The relationship between U_F, the generalized crack propagation force, $\mathcal{G}$, the global stress-intensity factor, K_I, and the Young's modulus E, is:

$$F = \int_0^\xi \mathcal{G}bhdy = \int_0^\xi \frac{K_I^2}{E} bhdy. \tag{9}$$

For a low fiber volume ratio, E can represent either the matrix or the composite material, and therefore:

$$\phi = \frac{1}{E} \frac{\partial}{\partial M} \int_0^\xi \left(K_{IM}^2 - \sum_{i=1}^{m} K_{Ii} - K_{I\sigma} \right)^2 bhdy. \tag{10}$$

If the crack is assumed at the onset of propagation, from eqs (1-3) and (10) we may obtain the constitutive relation between the localized rotation and the dimensionless moment of crack propagation:

$$\phi = \frac{2K_{IC}}{Eh^{0.5}} \left\{ \frac{M_F}{K_{IC}h^{1.5}b} \int_0^\xi Y_M^2(y)dy \right. \tag{11}$$

$$- \frac{N_P^{(1)m}}{\rho} \sum_{i=1}^{m} \left[\frac{P_i}{P_{P_i}} \rho_i \int_{\zeta_i}^\xi Y_M(y)Y_P(y, \zeta_i)dy \right]$$

$$\left. - N_P^{(2)} \int_0^\xi \left(\int_\zeta^\xi \frac{\sigma(w(y))}{\sigma_u} Y_M(y)Y_P(y, \zeta)dy \right) d\zeta \right\}$$

For a generical relation $\sigma(w)$, the fiber closing tractions onto the crack are indeterminate and depend on the unknown crack opening displacement function $w(x)$. The crack profile (fig.2) can be defined as a function of the mechanical and geometrical properties of the cross-section and of the applied loads, once again through Castigliano's Theorem:

$$w(\zeta_k) = \lim_{F \to 0} \frac{\partial}{\partial \zeta_k} \int_0^\xi \frac{K_I^2}{E} bhdy \ , \tag{12}$$

where $w(\zeta_k)$ is the crack opening displacement at the generic coordinate $\zeta = \zeta_k$, F are two fictitious opening
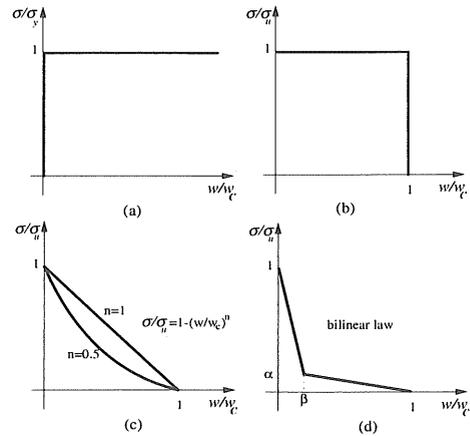

Figure 3. (a) Rigid-perfectly plastic law for primary reinforcement; (b) plastic law with vertical drop; (c) exponential softening law; (d) bilinear softening law for secondary reinforcement.

forces applied in ζ_k and K_I is the global stress-intensity factor:

$$K_I = K_{IM} - \sum_{j=1}^{m} K_{Ij} - K_{I\sigma} + K_{IF} \; , \tag{13}$$

in which K_{IF} is the stress-intensity factor due to the forces F. The normalized crack opening displacement assumes the following form, by substituting the expressions of the stress-intensity factors:

$$\tilde{w}(\zeta_k) = \frac{w(\zeta_k)}{h} = \frac{2K_{IC}}{Eh^{0.5}} \left\{ \frac{M}{K_{IC}h^{1.5}b} \int_{\zeta_k}^{\xi} Y_M(y) Y_P(y, \zeta_k) dy - \frac{N_P^{(1)}}{\rho} \sum_{i=1}^{m} \left[\frac{P_i}{P_{P_{imax}[\zeta_i, \zeta_k]}} \rho_i \int_{\zeta_k}^{\xi} Y_P(\zeta_i, y) Y_P(y, \zeta_k) dy \right] \right. \tag{14}$$
$$\left. - N_P^{(2)} \int_{\zeta_k}^{\xi} \left(\int_0^y \frac{\sigma(w(\zeta))}{\sigma_u} Y_P(y, \zeta) d\zeta \right) Y_P(y, \zeta_k) dy \right\}$$

in which the last term represents the displacement at the abscissa ζ_k due to the distribution of tractions $\sigma(w)$ between 0 e ξ. Equations (11) and (14) set up a statically indeterminate nonlinear problem. The reactions P_i and $\sigma(w)$ are evaluated by using a numerical procedure based on the assessment of kinematical compatibility and statical equilibrium equations. The complete description of the computational algorithm is reported in Section 4.

3 DIMENSIONAL ANALYSIS

The analytical formulation has been developed in a dimensionless form to define the parameters that synthetically control the behaviour of the cross-section in bending. A fundamental set of dimensionally independent variables, K_{IC} $[F][L]^{-1.5}$ and h $[L]$, has been chosen. The dimensionless products proposed in the theoretical formulation, $K_{IC}/(\sigma_u h^{0.5})$ and $M_F/(K_{IC} h^{1.5}b)$, have been obtained by multiplying the different variables involved in the physical problem by a suitable combination of the fundamental set.

The number of dimensionless parameters controlling the mechanical behaviour depends at first on the assigned bridging or cohesive relation $\sigma(w)$. If this relation is rigid-plastic, fig 3.b, the closing tractions are uniform and constant along the fictitious crack faces during the entire loading process. In the absence of the primary reinforcement, the traction-free crack depth ξ_r is equal to the depth of an initial notch. In that case, the constitutive flexural relationship can be evaluated through the equilibrium condition alone (Capinteri and Massabò, 1997b). If the geometrical ratios are kept constant, the brittleness number $N_P^{(2)}=1/s$ proves to be the single parameter controlling the kind of behaviour of the cross-section.

When, instead, the two reinforcement phases are present, and a generic bridging or cohesive law with a critical crack opening displacement w_c are considered, the problem is statically indeterminate and compatibility must be satisfied. To define the parameters controlling the behaviour for the above assumption, in addition to relations (5) and (11) reference must be done to the propagating condition for the traction-free crack, which controls the advancement of the bridging or cohesive zone. The presence of the primary reinforcement, complicates the problem, as at any interval between two bars, a zone with crack opening displacement greater than the critical value can be found (fig. 2). The traction-free crack propagates when the crack opening displacement reaches the critical value w_c. If $\tilde{E} = (Eh^{0.5})/K_{IC}$ is the dimensionless Young's modulus, eq.(14) yields:

$$\frac{M}{K_{IC}h^{1.5}b} \int_{\zeta_k}^{\xi} Y_M(y) Y_P(y, \zeta_k) dy - \frac{N_P^{(1)}}{\rho} \sum_{i=1}^{m} \left[\frac{P_i}{P_{P_{imax}[\zeta_i, \zeta_k]}} \rho_i \int_{\zeta_k}^{\xi} Y_P(\zeta_i, y) Y_P(y, \zeta_k) dy \right] \tag{15}$$
$$- N_P^{(2)} \int_{\zeta_k}^{\xi} \left(\int_0^y \frac{\sigma(w(\zeta))}{\sigma_u} Y_P(y, \zeta) d\zeta \right) Y_P(y, \zeta_k) dy = \frac{1}{2} \tilde{E} \tilde{w}_c$$

This condition is verified at each iteration of the procedure described in the previous section. It points to the fact that, for an assigned generic bridging or cohesive law, if geometrical similarity is assumed, another dimensionless parameter,

$$\tilde{w}_c^E = \tilde{E} \tilde{w}_c = \frac{Ew_c}{K_{IC}h^{0.5}} , \tag{16}$$

controls the composite flexural response. The functional constitutive relationship can be given the general form:

$$f\left(\frac{M}{K_{IC}h^{1.5}}, \phi, N_P^{(1)}, N_P^{(2)}, \tilde{w}_c^E \right) = 0 . \tag{17}$$

This relation has a general validity for both model options. Nevertheless, for the cohesive option, the brittleness number $N_P^{(2)} = 1/s$ and the parameter $\tilde{w}_c^E$ are not independent variables. This is due to the relationship holding between the homogenized fracture toughness of the matrix and the secondary phase reinforcement, given by K_{IC} in the cohesive option and the fracture energy $\mathcal{G}_F$:

$$\mathcal{G}_F = \int_0^{w_c} \sigma(w) dw \quad \text{where} \quad K_{IC} = \sqrt{\mathcal{G}_F E} . \tag{18}$$

The post-peak nonlinear matrix (matrix+fibers) fracture toughness is, in other words, linked, through Irwin's relationship, to the composite fracture energy, which is defined by the area beneath the cohesive

curve $\sigma(w)$. If the cohesive law $\sigma/\sigma_u = 1-(w/w_c)^n$ is assumed (fig.3.c), the following relationship holds:

$$\frac{K_{IC}^2}{E} = \int_0^{w_c} \sigma(w)\mathrm{d}w = \frac{n}{n+1}\sigma_u w_c.\qquad(19)$$

By means of eq.(20), the dimensionless parameter $\tilde{w}_c^E$ of eq. (17) can be expressed as a function of the brittleness number s, and the relation is:

$$\tilde{w}_c^E = \frac{n+1}{n}\frac{s}{E}.\qquad(20)$$

In the case of the bilinear law (fig.3.d), the relation between $\tilde{w}_c^E$ and s is the following:

$$\tilde{w}_c^E = s\frac{2}{\beta+\alpha}.\qquad(21)$$

As a consequence, the dimensional functional relationship (17) for the cohesive model becomes:

$$f(\tilde{M}, \phi, N_P^{(1)}, N_P^{(2)}) = 0,\qquad(22)$$

where $N_P^{(1)}$ and $N_P^{(2)}$ are the governing parameters.

In conclusion, if the theoretical problem is analyzed via the bridging option of the proposed model, and the material is modeled as multiphase, three parameters, $N_P^{(1)}$, $N_P^{(2)}$ and $\tilde{w}_c^E$ control the mechanical response of the cross-section. On the other hand, if the theoretical problem is analyzed via the cohesive option, which omogenizes the composite material, two parameters $N_P^{(1)}$ and $N_P^{(2)}$ affect the kind of structural response. Physical similitude in the structural response is predicted when the mechanical and geometrical properties vary, as long as the dimensionless parameters are kept constant.

4 ALGORITHM DESCRIPTION

The computation of the bending moment M_F and of the relative rotation between the faces of the crack ϕ for a given crack depth ξ is carried out by using the following fundamental relationships:

$$\begin{aligned}\{P\} &= \{P(\{w\},\sigma)\} \\ \{w\} &= \{w(\{P\},\sigma)\} \\ w(\zeta) &= w(\zeta,\{P\},\sigma)\end{aligned}\qquad(23)$$

These equations give respectively:
• the tractions at the m primary reinforcements (bars) as functions of the openings at the points where they are located and of the cohesive closing stresses;
• the openings at the primary reinforcements as functions of their tractions and of the cohesive closing stresses;
• the opening at a generic abscissa ζ as a function of the primary reinforcement tractions and of the cohesive closing stresses.
It is to be noted explicitly that the first two equations

(23) are not one the inverse of the other even in the non-cohesive case, i.e. even if $\sigma(\zeta) = 0 \;\forall\zeta \in [0,\xi]$. This is a consequence of the rigid plastic constitutive law for the primary reinforcements, stating that for the ith reinforcement it is $w(\zeta_i) = 0$ if $P_i < P_{P_i}$ and $w(\zeta_i) = w(\zeta,\{P\},\sigma)$ if $P_i = P_{P_i}$.
The iterative algorithm for implementing the model is structured on a two level computation:
• an external iteration computing the tractions and the openings at the m primary reinforcements;
• an internal iteration computing the distribution and extension of the cohesive intervals.

External iteration
In the external iteration the tractions/openings at the reinforcement bars are determined according to their rigid-plastic costitutive law for a given crack depth ξ and for some assumed distribution of the closing stresses along the crack faces. This distribution is updated in the internal iteration according to the costitutive law for the matrix/secondary reinforcement. The following description of the iteration algorithm is general, and applies to the three cases:
• only primary reinforcement is present $(N_P^{(1)} \neq 0, N_P^{(2)} = 0)$;
• only secondary reinforcement is present $(N_P^{(1)} = 0, N_P^{(2)} \neq 0)$;
• both primary and secondary reinforcement are present $(N_P^{(1)} \neq 0, N_P^{(2)} \neq 0)$.
A loop is performed over the m primary reinforcements, from the farthest to the closest to the crack tip. If the stress level at a certain reinforcement exceeds the maximum, then at this reinforcements the maximum stress is assigned and the relevant opening is computed. These assigned and computed data are used to recompute the stresses in the bars closest to the tip. The detailed flow follows:
1. Initialization;
2. if $N_P^{(2)} \neq 0$ the extension of the cohesive intervals is set to all;
3. if $N_P^{(1)} \neq 0$ the openings at the m primary reinforcements are set equal to zero, $\{w\} = \{0\}$, and a convergence tolerance tol_e is fixed;
4. Loop (the apex (k) indicates the kth iteration);
   (a) the stresses at the primary reinforcements are computed, $\{P\}^k = \{P(\{w\},\sigma)\}$;
   (b) the stresses exceeding or nearby the maximum are set equal to $P_i = \min(P_i + tol_e, P_P) \; i = 1....m$. Here the role of the tolerance tol_e is to eliminate the observed oscillations in the convergence process;
   (c) the current value of the tractions $\{P\}^{(k)}$ is used to compute the norm of the variation of the primary reinforcements stresses $\aleph_e = \|\{P\}^{(k)} - \{P\}^{(k-1)}\|_{+\infty}$. The (plus infinity) norm $\|\;\|_{+\infty}$ is defined as the maximum absolute value in the components of the argument vector;

(d) if $N_P^{(2)} \neq 0$ then go to the internal iteration for the computation and updating of the distributed closing stresses (secondary reinforcement);

(e) loop exiting condition in the case $N_P^{(2)} \neq 0$, $N_P^{(1)} = 0$. In this case, as no interaction is present with the primary reinforcement (it being absent) and all the computations are carried out in the internal iteration, the loop is exited immediately;

(f) loop convergence check in the case $N_P^{(2)} \neq 0$, $N_P^{(1)} \neq 0$. If $\aleph_e < tol_e \|\{P_P\}\|_{+\infty}$, the algorithm has converged and the loop is exited;

(g) loop for $i = 1....m$ (openings and primary reinforcements tractions update);

    (g.1) if $P_i^{(k))} = P_{P_i}$ then compute the opening $w(\zeta_i) = w(\zeta_i, \{P\}^{(k)}, \sigma)$ and recompute the stresses at the primary reinforcements, $\{P\}^{(k)} = \{P(\{w\}, \sigma)\}$ else $w(\zeta_i) = 0$ and $P_i^{(k)} = \max(0, P_i^{(k)})$;

    (g.2) set $P_i^{(k)} = \min(P_i^{(k)}, P_{P_i})$;

(h) end loop i;

(i) $\aleph_e = \|\{P\}^{(k)} - \{P\}^{(k-1)}\|_{+\infty}$

(j) loop convergence check in the case $N_P^{(1)} \neq 0, N_P^{(2)} = 0$. If $\aleph_e < tol_e \|\{P_P\}\|_{+\infty}$ the algorithm has converged and the loop is exited;

5. return to step 4.

Internal iteration

For a fixed value of the tractions at the primary reinforcements and of the corresponding openings $\{w\}$ the internal iteration computes the extension of the cohesive intervals and applies the secondary reinforcement (or matrix) constitutive law. The extension of the cohesive intervals is determined by a couple of abscissas for each primary reinforcement, setting the related lower and upper limit of the cohesive interval. The crack tip is treated algorithmically in the same way, in the sense that it has associated a couple of cohesive abscissas. The lower represents the extension of the cohesive interval below the crack tip, and the second is always coincident with the crack tip itself, fig. 2. Consequently, the number of interval extrema is globally $2m+2$, m being the number of primary reinforcements, and the $m+1$ cohesive intervals are determined by $[\{z_c\}_{i-1}, \{z_c\}_i]$ $i = 2, 4, ..., 2m+2$. Here $\{z_c\}$ is the vector storing the abscissas, and it is always sorted in ascending order: $\{z_c\}_i \leq \{z_c\}_{i+1}$ $i = 1, ..., 2m+1$. Note that the functions defined over the cohesive intervals, e.g. displacements and cohesive stresses $\sigma(w)$, are non differentiable at the points where the primary reinforcements are located and consequently care must be exerted in computing the quadratures.

In the general case, the equation $\{w\} = \{w(\{P\}, \sigma)\}$ is an integral equation, σ being a function of the opening by the constitutive law, $\sigma = \sigma(w)$. For this reason the stresses are computed considering the displacements at the previous iteration. When convergence is reached, the difference between the two is, of course,

negligible. The crack is subdivided into $m+1$ zones where the displacement is a continuous and differentiable function to store the displacements at the previous iteration. In the case of a single primary reinforcement ($m=1$) the first zone extends from the abscissa zero to the one of the first primary reinforcement z_1, and the second zone extends from z_1 to the crack tip ξ. Into each zone the displacements are stored in the form of a spline interpolation. The spline interpolation w_s computed at an iteration is used in the subsequent iteration to approximate the closing stresses through the constitutive relation $\sigma = \sigma(w) \cong \sigma(w_s)$. This approach is an evolution of the one proposed by Carpinteri and Massabò (1997a), where a simple spline was used to interpolate the closing stresses σ. In the present case difficulties arise because the concavity of the interpolation may contradict one of the data, especially when nondifferentiable constitutive laws are used.

The internal iteration algorithm described in the following is a form of the binary search (bisection) algorithm on the abscissas of the cohesive intervals $\{z_c\}$ applied to each of the $m+1$ zones in wich the crack is subdivided. The ith zone contains the superior extremum z^s of the $(i-1)^{th}$ interval and the inferior extremum z^i of the ith interval. Two convergence measures are evaluated: $\aleph_z = \|\{z_c\}^{(k-1)} - \{z_c\}^{(k)}\|_{+\infty}$ accounting for the variation of the cohesive intervals between two subsequent iterations, and $\aleph_s = \|\{w_s(\{z_c\})\}^{(k)} - \{w(\{z_c\})\}\|_{+\infty}$ accounting for the precision of the spline interpolation vs. the exact displacement measured at the extrema of the cohesive intervals.

The internal iteration loop structure is the following:

1. compute the spline concavity preserving interpolation on the $m+1$ zones;

2. loop over the $m+1$ zones, from the closest to the crack tip to the farthest;

    (a) if $w(z^s) < w_c$ then the cohesive interval is enlarged by bisection on the right, else the cohesive interval is reduced by bisection on the left;

    (b) if $w(z^i) < w_c$ then the cohesive interval is enlarged by bisection on the left, else the cohesive interval is reduced by bisection on the right;

3. end loop on the zones;

4. the vector $\{z_c\}$ is sorted in ascending order. This is necessary because the abscissas updating by bisection can produce overlapping cohesive intervals, which are eliminated in this step;

5. compute the norms $\aleph_z$ and $\aleph_s$ and check for the convergence condition;

6. if not converged go to step 1.

5 SIMULATIONS AND SIZE-SCALE EFFECT

In the flexural behaviour of reinforced concrete with a nonlinear matrix, a size-scale effect can be evi-

denced. This effect consists of variations in the shape of the constitutive relationship when a characteristic dimension of the body varies. This aspect, as previously mentioned, is very important when experimental results obtained on small specimens have to be extrapolated to full scale structures. In fact, for high strength concrete with fibers and with high primary reinforcement percentage, it results very hard to perform experimental tests on full size elements.

To analyze this phenomenon, the bridging option of the proposed theoretical model has been applied assuming for the secondary reinforcement the bridging relation, $\sigma(w)=\rho\sigma_u$ if $w=w_c$ and $\sigma(w)=0$ if $w>w_c$. The flexural behaviour of the cross-section is controlled by the three parameters $N_P^{(1)}$, $N_P^{(2)}$ and $\tilde{w}_c^E$. If only the size-scale effect is of interest, the mechanical properties can be assumed constant (K_{IC}, E, $\rho\sigma_y$, $\gamma\sigma_u$, w_c). The two products of the two brittleness numbers $N_P^{(1)}$, $N_P^{(2)}$ times $\tilde{w}_c^E$:

$$N_P^{(1)}\tilde{w}_c^E = \frac{\rho\sigma_y w_c}{\mathcal{G}_F} = \frac{\rho\sigma_y E w_c}{K_{IC}^2} \qquad (24)$$

$$N_P^{(2)}\tilde{w}_c^E = \frac{\gamma\sigma_u w_c}{\mathcal{G}_F} = \frac{\gamma\sigma_u E w_c}{K_{IC}^2}$$

which do not depend on the depth of the cross-section, are fixed.

Table 1: Dimensionless parameters by varying h.

h (mm)	$N_P^{(1)}$	$N_P^{(2)}$	$\tilde{w}_c^E$
10	0.119	0.054	1482
20	0.168	0.077	1048
50	0.265	0.121	663
100	0.375	0.172	469
500	0.839	0.384	210
1000	1.186	0.544	148

In order to show the effect of element size on the flexural response, the following example has been analyzed. Let consider six geometrically similar elements, with h between 10 and 1000 mm. The beams are characterized by a single reinforcement bar applied at $0.1\,h$ from the bottom of the beam, with reinforcement ratio equal to 1% and yield stress $\sigma_y =240$ Nmm^{-2}, elastic modulus $E = 30000$ Nmm^{-2}, cementitious matrix toughness $K_{IC} = 64$ Nmm$^{-3/2}$, and with 1% in volume ratio of fibers embedded in the matrix ($\sigma_u =110$ Nmm^{-2}). With these mechanical parameters the two ratios of eq. (24) assume respectively the values: 187 the former and 86 the latter.

By varying h, the three dimensionless parameters assume the values reported in Tab.1. The evolutive process of crack propagation expressed in terms of the dimensionless crack propagation moment, $M_F/(K_{IC}h^{1.5}b)$, vs the normalized crack depth, $\xi=a/h$, for

the six cases is reported in fig.4.a. For $0<\xi<\zeta_1$, the crack crosses only the matrix of the cross-section. The strain-softening response is controlled by the matrix toughness and by the secondary reinforcements. For crack depths tending to zero, an infinite resistance is provided, as expected form LEFM.

In correspondence of $\xi=\zeta_1=0.1$, when the crack reaches the primary reinforcement, a loading drop is evidenced. For the smallest sizes, the response is unstable and an uncontrollable crack propagation can be avoided only by decreasing the applied load. On the other hand, for the largest sizes, the process is stable, and a slow crack growth is possible also by increasing the applied load. The crack propagation moment vs local rotation diagram is reported in fig. 4.b. The crack propagation moment shows a vertical asymptote for $\phi\to 0$ ($\xi\to 0$). A vertical drop is achieved when the crack crosses the primary reinforcement. A
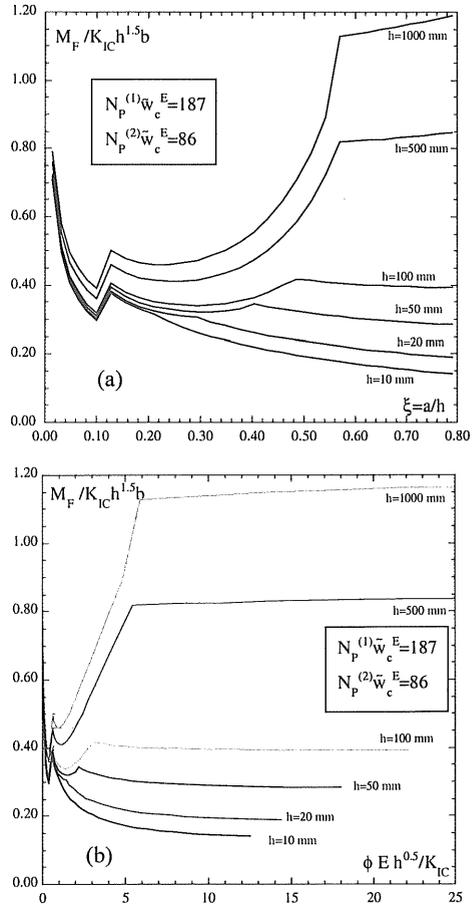

Figure 4. (a) Dimensionless crack propagation moment vs normalized crack depth for beam depth varying between 10 and 1000 mm. (b) Dimensionless crack propagation moment vs normalized local rotation.

snap-through instability is present after the drop (dotted line), for $h{\geq}100$ mm, which is less and less evident for increasing size and an evident hardening portion develops. On the other hand, for $h=20$ and 10 mm the flexural behaviour is brittle, and a monotonically decreasing branch follows the peak moment.

Therefore, to predict the structural behaviour of an element with cross-section characterized by beam depth $h=500$ mm, bar reinforcement percentage equal to 1%, and fibers percentage of 1% by experimental test on a beam scaled 1:10 ($h=50$ mm), the scaled beam must have a steel percentage equal to 3.16% and a fiber reinforcement ratio of 3.16% in order to have the same flexural behaviour. In other words, the reinforcement percentage, as well as the fiber percentage, when the other mechanical parameters are fixed, must be scaled as $h^{0.5}$, so that the brittleness numbers remain the same.

CONCLUSIONS

The proposed model represents an extension of the bridged crack model to the concurrent presence in a cementitious matrix of longitudinal bars and uniformly distributed fibers. A cohesive crack version has also been considered. It has been shown that the flexural behaviour of geometrically similar structures is governed by three dimensionless parameters. The model reproduces the structural behaviour of high-performance and/or fiber reinforced concrete members in bending. In particular, as the governing parameters are of easy physical meaning and of simple experimental evaluation, this model represents a very useful tool for the study of mechanical properties (strength and ductility) and of crack propagation regimes, according to concrete composition, typology and density of the fibers, distribution and characteristics of the longitudinal bars. A very important result of the formulation is provided by the dependence of the structural behaviour on the member size. Only with the same brittleness numbers it is possible to obtain physically similar structural responses.

ACKNOWLEDGEMENTS

REFERENCES

Barenblatt, G.I., 1962. The mathematical theory of equilibrium cracks in brittle fracture. In Dryden, H.L., von Karman, T. (Eds.), Advances in Applied Mechanics, Academic Press, New York, pp.55-129.

Bosco, C., Carpinteri, A., 1992. Softening and snap-through behavior of reinforced elements. Journal of Engineering Mechanics (ASCE) 118: 1564-1577.

Bosco, C., Carpinteri, A., 1995. Discontinuous constitutive response of brittle matrix fibrous composites. Journal of the Mechanics and Physics of Solids 43: 261-274.

Buckingham, E., 1915. Model experiments and the form of empirical equations. Transactions ASME 37: 263-296.

Carpinteri, A.,1981. Static and energetic fracture parameters for rocks and concrete. Materials and Structures 14: 151-162.

Carpinteri, A.,1984. Stability of fracturing process in RC beams. Journal of Structural Engineering (ASCE) 110: 544-558.

Carpinteri, A., Ferro, G., Ventura, G., 2000. The bridged crack model for the analysis of fiber-reinforced composite materials. In: de Wilde, W.P., Blain, W.R., Brebbia, C.A. (Eds.) Composite Materials & Structures: 301-310, WIT Press, Southampton.

Carpinteri, A., Ferro, G., Bosco, C. & Elkathieb, M., 1999. Scale effects and transitional phenomena of reinforced concrete beams. In: Carpinteri, A. (Ed.). Minimum Reinforcement in Concrete Members, Elsevier Science, Oxford, pp.1-30.

Carpinteri, A., Massabò, R., 1996. Bridged versus cohesive crack in the flexural behavior of brittle-matrix composites. International Journal of Fracture 81: 125-145.

Carpinteri, A., Massabò, R., 1997a. Continuous vs discontinuous bridged-crack model for fiber-reinforced materials in flexure, International Journal of Solids and Structures 34: 2321-2338.

Carpinteri, A., Massabò, R., 1997b. Reversal in failure scaling transition of fibrous components. Journal of Engineering Mechanics (ASCE) 123: 107-114.

Cox, B.N., Mashall, D.B., 1994. Concepts for bridged cracks in fracture and fatigue. Acta Metallurgica et Materialia 42: 341-363.

Jenq, Y.S., Shah, S.P., 1986. Crack propagation in fiber-reinforced concrete. Journal of Engineering Mechanics (ASCE) 112: 19-34.

Mashall, D.B. Cox, B.N., Evans, G.A., 1985. The mechanics of matrix cracking in brittle-matrix fiber composites. Acta Metallurgica et Materialia 33: 2013-2021.

Noghabai, K., 2000. Beams of fibrous concrete in shear and bending: experiment and model. Journal of Structural Engineering (ASCE) 126: 243-251.

Okamura, H., Watanabe, K., Takano, T., 1975. Deformation and strength of cracked member under bending moment and axial force. Engineering Fracture Mechanics 7: 531-539.

Tada, H., Paris, P.C., Irwin, G., 1963. The Stress Analysis of Cracks Handbook. Paris Productions Incorporated (and Del Research Corporation), St. Louis, Missouri.

Willis, J.R., 1967. A comparison of the fracture criteria of Griffith and Barenblatt. Journal of the Mechanics and Physics of Solids 15: 151-162